RSC Advances

PAPER

View Article Online
View Journal | View Issue



Cite this: *RSC Adv.*, 2015, **5**, 86172

# Nitrogen functional groups on an activated carbon surface to effect the ruthenium catalysts in acetylene hydrochlorination†

Na Xu,[a] Mingyuan Zhu,*[ab] Jinli Zhang,*[ac] Haiyang Zhang[ab] and Bin Dai[ab]

Received 14th September 2015
Accepted 24th September 2015

DOI: 10.1039/c5ra18851b

www.rsc.org/advances

To improve the activity and stability of Ru-based catalysts with a carbon support for acetylene hydrochlorination, activated carbon (AC) was consecutively modified by nitration, amination and pyridine, and the effect of the different carbon supports on the Ru-based catalysts for acetylene hydrochlorination was investigated. The results of the FT-IR studies confirmed that $-NO_2$, $-NH_2$ and –N–H–N groups were separately grafted onto the surface of the AC. Under the same reaction conditions, the modified catalysts exhibited better catalytic activity compared with the original Ru/AC catalyst. Moreover, the catalyst Ru/AC-NHN showed the best catalytic performance with a slight decrease after 48 h from 93.2% to 91.8%. The increase in catalytic activity indicates that the modification with nitrogen functional groups is beneficial for acetylene hydrochlorination.

## 1. Introduction

The acetylene hydrochlorination reaction is an important process to synthesize vinyl chloride in industry. However, the catalyst used in the reaction is $HgCl_2$, which is highly toxic and causes serious environmental pollution. Therefore, it is imperative to explore non-mercury catalysts with high activity and long stability for acetylene hydrochlorination.

The pioneering works of Hutchings suggested that the activity of metal catalysts was associated with the standard electrode potentials of the related metal ions.[1] Accordingly, the $AuCl_3$ catalyst is the optimal catalyst with its high activity. In fact, although Ru is also a precious metal, it is low-cost compared to Au, and Ru-based catalysts have caused extensive research. However, the catalytic activity and stability of Ru-based catalysts still need to be further improved in the acetylene hydrochlorination process. Bimetallic Ru-Co/SAC resulted in good catalytic activity and coking inhibition capability.[2] Li *et al.* reported that Ru catalysts deposited inside CNT channels exhibited optimal catalytic activity, with an acetylene conversion of 95.0% and a selectivity to VCM of 99.9%.[3] Additionally, Pu *et al.* reported that the original Ru/SAC catalyst was oxidized under air at 300 °C for 1 h with the catalytic performance of stable acetylene conversion at 96.5% for 48 h at 170 °C and a $C_2H_2$ gas hourly space velocity (GHSV) of 180 $h^{-1}$.[4]

In the field of acetylene hydrochlorination, activated carbon is the best catalyst carrier. According to the previous report, the functional groups on an activated carbon surface will affect its catalytic activity. Recently, Zhao *et al.* successfully demonstrated that the doping of nitrogen can efficiently enhance the catalytic performance of Au/AC and Au-Cs/AC.[5,6] Wang *et al.* reported that a P-doped carbon support can also significantly enhance the catalytic activity of a Au/SAC catalyst for acetylene hydrochlorination.[7] Previous literature also reported that amino-functionalized metal–organic frameworks adsorbed pyridine *via* hydrogen bonding.[8] According to this understanding of previous work, there are no reports of the amination of activated carbon with pyridine adsorbed *via* hydrogen bonding for acetylene hydrochlorination.

Therefore, in this work, we prepared Ru-based catalysts supported on activated carbon, which was modified with $-NO_2$, $-NH_2$ and –N–H–N groups, and assessed their catalytic activity for acetylene hydrochlorination, aiming to improve the activity and stability of the acetylene hydrochlorination catalysts. In combination with characterization using TEM, TPR, XPS and FT-IR, *etc.*, it was indicated that Ru-based catalysts deposited on activated carbon modified by –N–H–N exhibited the highest catalytic activity for acetylene hydrochlorination.

## 2. Experimental

### 2.1. Materials

Activated carbon (neutral, coconut carbon) was purchased from Tangshan United Carbon Technology Co., Ltd; $RuCl_3$ (with 48.7% Ru content) and nitric acid (AR, 65.0–68.0%) were

[a]School of Chemistry and Chemical Engineering of Shihezi University, Shihezi, Xinjiang, 832000, PR China. E-mail: zhuminyuan@shzu.edu.cn; zhangjinli@tju.edu.cn; Fax: +86 993 2057210; +86-22-27890643; Tel: +86 993 2057270; +86-22-27890643
[b]Key Laboratory for Green Processing of Chemical Engineering of Xinjiang, Bingtuan, Shihezi, Xinjiang, 832000, PR China
[c]School of Chemical Engineering and Technology, Tianjin University, Tianjin, 300072, PR China

† Electronic supplementary information (ESI) available. See DOI: 10.1039/c5ra18851b

purchased from Tianjin Fengchuan Chemical Reagent Technology Co., Ltd; acetic anhydride (AR, ≥98.5%) was purchased from Tianjin Yongsheng Chemical Reagent Co., Ltd; pyridine (AR, ≥99.5%) was purchased from Tianjin Fuyu Fine Chemical Co., Ltd; aqua ammonia (AR, 25.0–28.0%) and sodium borohydride (AR, ≥97.0%) were purchased from Chengdu Kelong Chemical Reagent Company. All the other materials and chemicals were commercially available and were used without further purification.

### 2.2. Modification of AC samples

According to the previously reported method,[9] nitration modification of the AC sample was performed as follows: 30 mL of nitric acid was slowly dripped into a suspension of AC and 40 mL of acetic anhydride in a three-neck round bottom flask at room temperature. After stirring at this temperature for 24 h, the solid sample was filtrated and washed until the filtrate was neutral. The sample was dried at 110 °C for 14 h, and labeled as AC-$NO_2$.

Amination of the AC-$NO_2$ sample was carried out as follows: AC-$NO_2$ was mixed with 10 mL of ammonia solution and 20 mL of deionized water. After adding 0.75 g of sodium borohydride, the suspension was kept at room temperature for 24 h under stirring. The solid was filtrated, washed with deionized water until the filtrate was neutral, and then dried at 110 °C for another 24 h. The obtained sample was labeled as AC-$NH_2$.

Then 20 mL of pyridine was dripped into AC-$NH_2$ in a three-neck round bottom flask at room temperature. After stirring at this temperature for 24 h, the solid samples were filtrated and washed until the filtrate was neutral, and then dried at 110 °C for 14 h. The obtained sample was labeled as AC-NHN.

### 2.3. Preparation of Ru-based catalysts

The Ru-based catalysts were prepared *via* the incipient wetness impregnation method.[10] A $RuCl_3$ aqueous solution was quantitatively mixed with a modified carbon support under stirring to prepare the catalyst with a Ru loading content of 1 wt%. Then the catalyst was desiccated at 140 °C for 18 h. The obtained catalysts were labeled as Ru/AC, Ru/AC-$NO_2$, Ru/AC-$NH_2$ and Ru/AC-NHN.

### 2.4. Catalyst characterization

Low temperature $N_2$ adsorption–desorption experiments were performed with a Micromeritics ASAP 2020 instrument to investigate the surface area and porosity. Fourier-transform infrared spectroscopy (FT-IR) was used to judge the functional group changes with Harrick's Praying Mantis diffuse reflection attachment. Transmission electron microscopy (TEM) was performed with a JEM2010 electron microscope at an accelerating voltage of 200 kV. X-ray diffraction (XRD) patterns were collected using a Bruker D8 advanced X-ray diffractometer with Cu-Kα irradiation ($\lambda$ = 1.5406 Å) at 40 kV and 40 mA at wide angles (10–90° in 2$\theta$). Temperature-programmed reduction (TPR) measurements were performed using a TPDRO 1100 (Thermo-Finnigan) instrument equipped with a thermal conductivity detector (TCD). The weight of the tested samples was 100 mg. Prior to each test, the samples were treated with $N_2$ gas at 60 °C for 1 h. After cooling, the temperature was increased from 30 to 800 °C at a heating rate of 10 °C $min^{-1}$ with a 10.0% $H_2$/Ar atmosphere flowing at a rate of 40 mL $min^{-1}$. Temperature-programmed desorption (TPD) was also analyzed using TPDRO 1100 apparatus at a temperature ramp of 25–400 °C with a ramp rate of 10 °C $min^{-1}$ and a flow rate of 45 mL $min^{-1}$. The final temperature of 400 °C was maintained for 20 min. X-ray photoelectron spectroscopy (XPS) data were recorded using an Axis Ultra spectrometer equipped with a monochromatized Al-Kα X-ray source (225 W).

### 2.5. Catalytic performance tests

The catalytic performance tests for acetylene hydrochlorination were carried out in the fixed-bed reactor (i.d., 10 mm). A purge pipeline with nitrogen was used prior to the catalytic reaction to remove any water and air in the system. Then the catalyst (2 mL) was activated with hydrogen chloride (gas, 99%) at a flow rate of 20 mL $min^{-1}$. After the reactor was heated to 180 °C, acetylene (11.8 mL $min^{-1}$) and hydrogen chloride (13.5 mL $min^{-1}$) were fed through the heated reactor to achieve a GHSV ($C_2H_2$) of 360 $h^{-1}$, which contained 2 mL of catalyst. The reaction products were analyzed by gas chromatography (GC-2014C).

## 3. Results and discussion

The catalytic performance of the catalysts and the supports are shown in Fig. 1. It can be seen that the supports (AC, AC-$NO_2$, AC-$NH_2$ and AC-NHN) exhibit relatively low activity for the acetylene hydrochlorination (Fig. 1a). Compared with the original Ru/AC catalyst, the catalytic activity and stability of the Ru-based catalysts (Ru/AC-$NO_2$, Ru/AC-$NH_2$ and Ru/AC-NHN) are greatly enhanced when the AC is modified with nitrogen functional groups, and the initial acetylene conversion increases as the activated carbon is decorated consecutively, achieving the highest value of 93.2% over the Ru/AC-NHN catalyst with no obvious decline after 48 hours of reaction. All of these related catalysts show the selectivity to VCM at above 99.0% at 48 h (Fig. 1b and d). This result indicates that the presence of nitrogen functional groups, especially –NHN, promotes the initial catalytic activity of the Ru-based catalysts and significantly enhances the catalyst stability.

The FT-IR spectra of the supports AC, AC-$NO_2$, AC-$NH_2$ and AC-NHN are shown in Fig. 2. Compared with AC, AC-$NO_2$ shows a characteristic peak at 1328 $cm^{-1}$, which is assigned to the fundamental vibration of the –$NO_2$ group.[11] However, the peak disappears after further amination of the AC-$NO_2$ support, and for the AC-$NH_2$ support, the peaks at 3744 and 1521 $cm^{-1}$ are assigned to the vibrations of $NH_2$ and NH in the amine groups, respectively.[12] Further, the characteristic peak of NH has shifted to a lower wavelength (1508 $cm^{-1}$) and a new peak at 2987 $cm^{-1}$ has appeared in the AC-NHN spectrum. This is probably due to the action of hydrogen bonding, formed from pyridine accepting a proton from $NH_2$ to give a strong hydrogen bond.[13] Thus, the FT-IR results confirm that the nitrogen functional groups

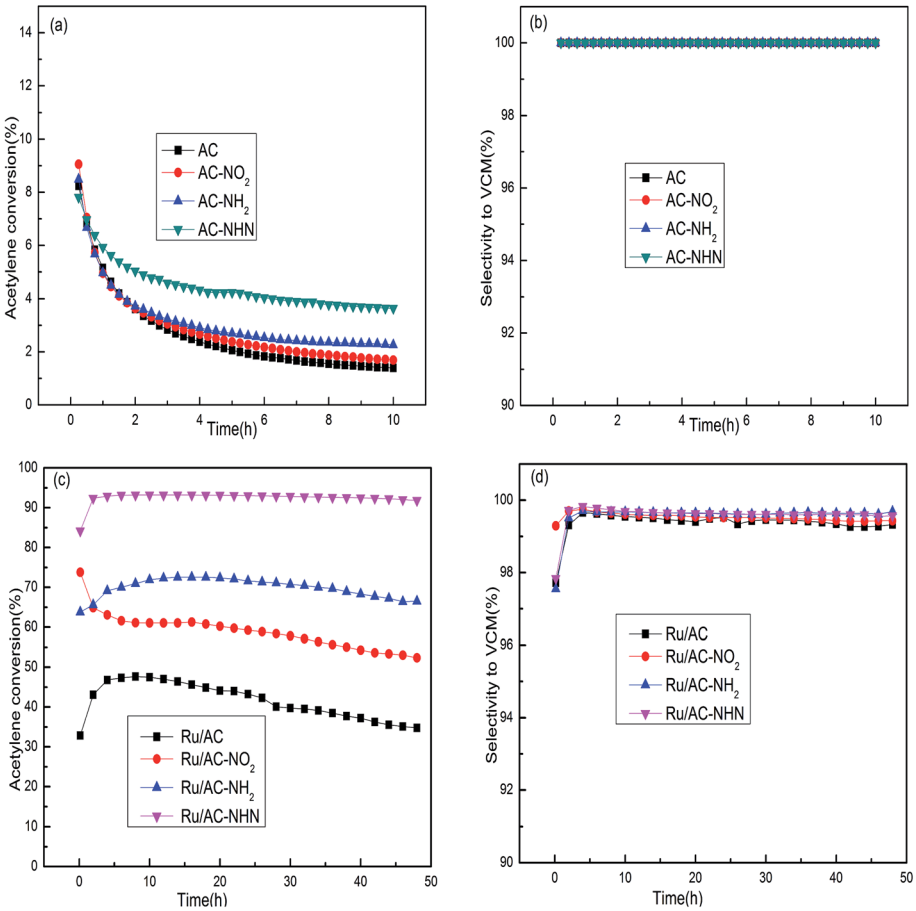


Fig. 1 Acetylene conversion (a and c) and selectivity (b and d) to VCM over the supports and the catalysts. Reaction conditions: temperature ($T$) = 180 °C, GHSV ($C_2H_2$) = 360 $h^{-1}$ and $V$(HCl)/$V$($C_2H_2$) = 1.15.

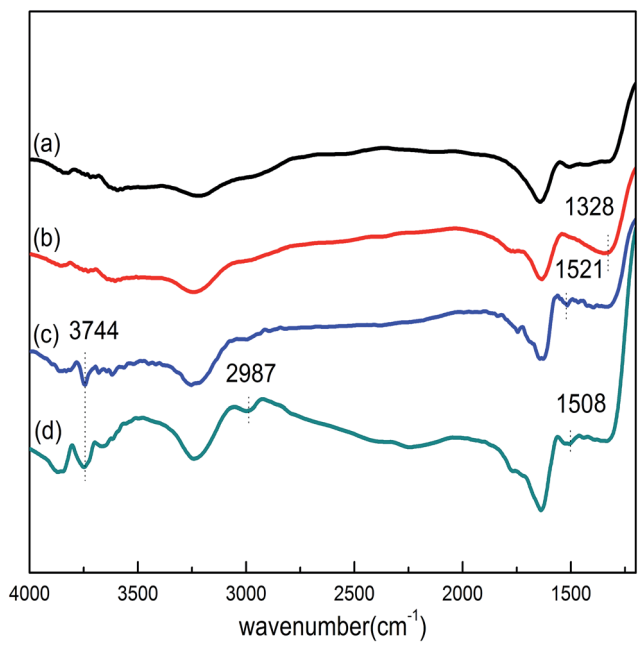


Fig. 2 FT-IR spectra of: (a) AC, (b) AC-$NO_2$, (c) AC-$NH_2$ and (d) AC-NHN.

Table 1 Elemental analysis for the supports

| | Element composition (%) | | |
|---|---|---|---|
| Samples | C | H | N |
| AC | 85.99 | 3.36 | 0.21 |
| AC-$NO_2$ | 78.77 | 3.59 | 0.73 |
| AC-$NH_2$ | 80.88 | 3.82 | 1.05 |
| AC-NHN | 82.57 | 3.51 | 1.67 |

Table 2 Physical properties of the different AC samples[a]

| Samples | $S_{BET}$ ($m^2$ $g^{-1}$) | $V$ ($cm^3$ $g^{-1}$) | $D$ (nm) |
|---|---|---|---|
| AC | 1030 | 0.57 | 2.20 |
| AC-$NO_2$ | 871 | 0.44 | 2.01 |
| AC-$NH_2$ | 933 | 0.52 | 2.25 |
| AC-NHN | 924 | 0.51 | 2.21 |

[a] $S_{BET}$: surface area; $V$: total pore volume; $D$: average pore diameter.

(–$NO_2$, –$NH_2$ and –NHN) were successfully grafted onto the surface of the AC in the consecutive modification steps.

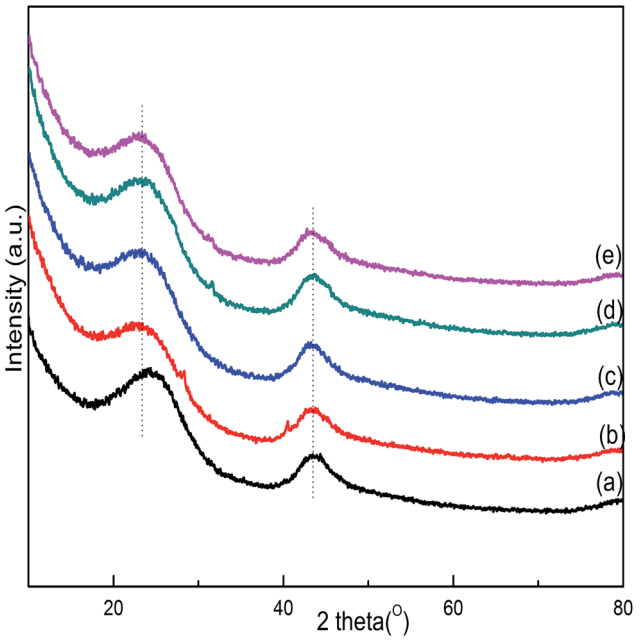


Fig. 3 X-ray diffraction patterns of (a) the AC support, and the fresh catalysts (b) Ru/AC, (c) Ru/AC-$NO_2$, (d) Ru/AC-$NH_2$ and (e) Ru/AC-NHN.

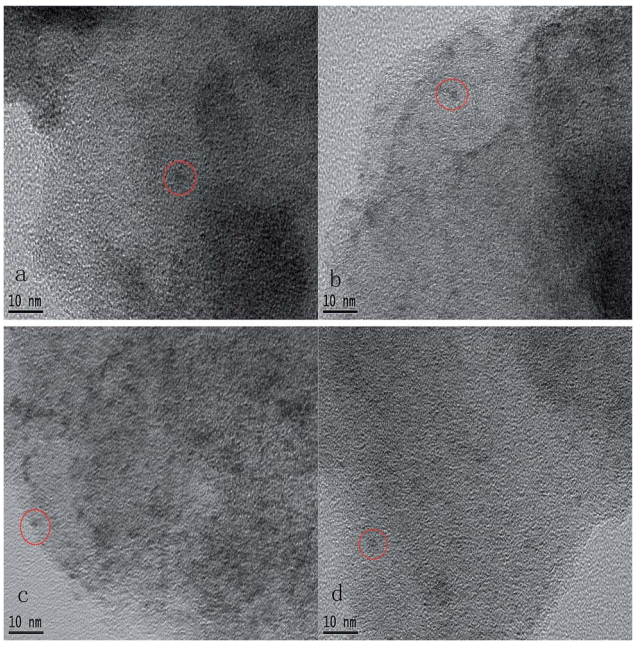


Fig. 4 TEM images of the fresh catalysts: (a) Ru/AC, (b) Ru/AC-$NO_2$, (c) Ru/AC-$NH_2$, and (d) Ru/AC-NHN.

Elemental analysis was carried out to determine the amount of nitrogen-containing groups grafted onto the activated carbon surface, the results are listed in Table 1. Only a trace amount of nitrogen is detected on AC, which possibly originates from weakly physisorbed nitrogen impurities on the surface.[14] Then the content of nitrogen increases gradually from 0.73% for AC-$NO_2$ to 1.67% for AC-HNH as the activated carbon was consecutively modified, indicating the presence of nitrogen-containing functional groups. Table 2 shows the specific surface area and total pore volume of the AC support before and after surface modification. The BET surface areas for AC, AC-$NO_2$, AC-$NH_2$ and AC-HNH are 1030, 871, 933 and 924 $m^2\ g^{-1}$, respectively. The pore volumes of AC, AC-$NO_2$, AC-$NH_2$ and AC-HNH are 0.57, 0.44, 0.52 and 0.51 $cm^3\ g^{-1}$, respectively. The decrease in the BET surface areas and pore volumes may also indicate that the functional groups were successfully grafted on the surface of the AC and that the pores were occupied by these groups after surface modification.[15,16]

Fig. 3 shows the XRD patterns of the AC, and the fresh catalysts Ru/AC, Ru/AC-$NO_2$, Ru/AC-$NH_2$ and Ru/AC-NHN. As

Table 3 Estimated Ru element dispersion in the catalysts determined by CO chemisorption

| Catalysts | CO uptake (μmol CO per g) | Ru dispersion (%) |
|---|---|---|
| Ru/AC | 76.54 | 80.58 |
| Ru/AC-$NO_2$ | 63.95 | 68.04 |
| Ru/AC-$NH_2$ | 50.12 | 51.17 |
| Ru/AC-NHN | 43.70 | 45.53 |

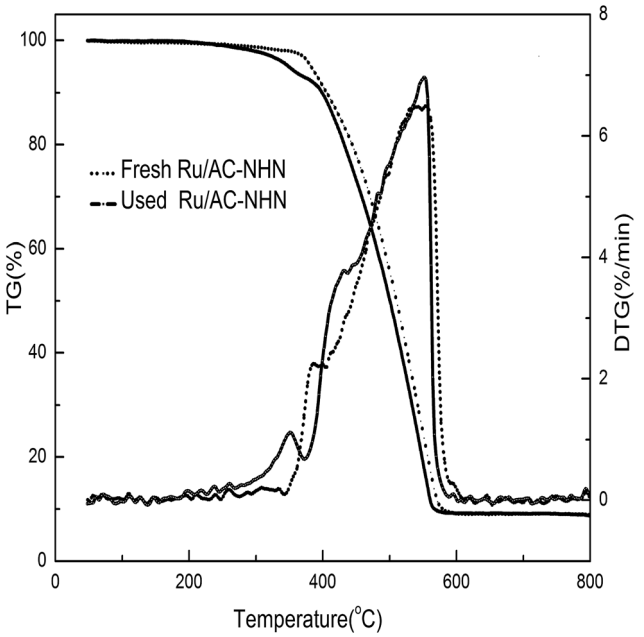


Fig. 5 TGA curves of the fresh and used catalysts of Ru/AC-NHN.

Table 4 Carbon deposition of the Ru-based catalysts

| Catalysts | Content of carbon deposition (%) |
|---|---|
| Ru/AC | 13.2 |
| Ru/AC-$NO_2$ | 6.8 |
| Ru/AC-$NH_2$ | 3.2 |
| Ru/AC-NHN | 1.9 |

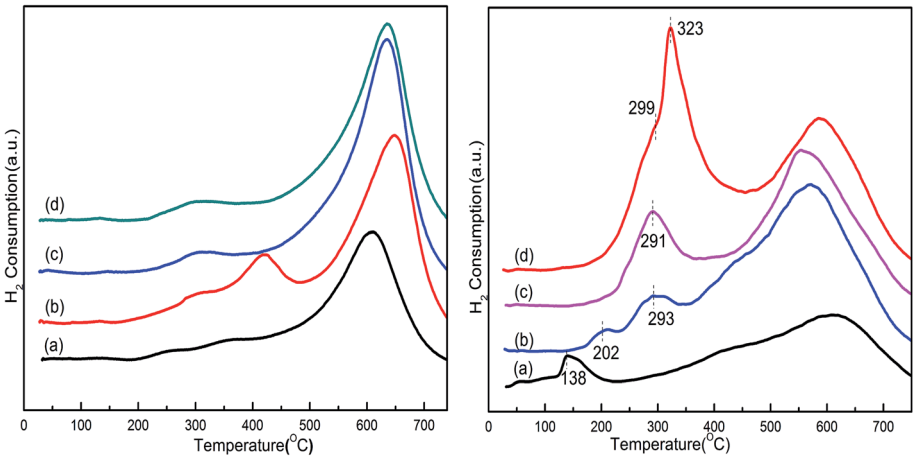


Fig. 6 TPR profiles of the supports: (a) AC, (b) AC-$NO_2$, (c) AC-$NH_2$ and (d) AC-NHN, and the catalysts: (a) Ru/AC, (b) Ru/$NH_2$, (c) Ru/AC-NHN, and (d) Ru/AC-$NO_2$.

Table 5 The relative areas of the $H_2$ consumption peaks for the catalysts

| Catalysts | $H_2$ consumption peaks (%) |
|---|---|
| Ru/AC | 4.16 |
| Ru/AC-$NO_2$ | 68.60 |
| Ru/AC-$NH_2$ | 6.64 |
| Ru/AC-NHN | 20.60 |

shown in Fig. 3, apart from the two obvious diffraction peaks at 23.4° and 43.5° originating from the (002) and (101) planes of AC, no discernible reflection of metallic Ru or anhydrous tetragonal $RuO_2$ is detected for any of the catalysts,[17] indicating a high dispersion of active species or a small particle size (< 4 nm).[18] In addition, the TEM images in Fig. 4 show that it is difficult to distinguish the homogeneous dispersion of small and uniform Ru particles. This may be due to a high dispersion of the Ru particles, which is consistent with the XRD results. Moreover, the dispersion of the Ru elements was estimated by CO chemisorption experiments.[19] As listed in Table 3, the Ru dispersion is 80.58% for the Ru/AC catalyst. However, the Ru dispersion decreases after modification with the nitrogen functional groups, with a lowest dispersion of 45.53% achieved for the Ru/AC-NHN catalyst, followed by Ru/AC-$NH_2$ (51.17%) and Ru/AC-$NO_2$ (68.04%). Thus, the modification of activated carbon is not beneficial to improve the dispersion of the catalyst.

TGA analysis was carried out to measure the amount of carbon deposition, and the results are shown in Fig. 5. In the case of the Ru/AC-HNH catalyst, both the fresh and the used catalysts have a slight weight loss before 150 °C owing to the desorption of adsorbed water (Table S1†). In the temperature range of 150–400 °C, there is an obvious weight loss (10.0%, Table S1†) for the used catalyst. When the temperature exceeds 400 °C, there appears to be a rapid weight loss mainly due to the combustion of the activated carbon. Thus, the coke burning may occur in the temperature range of 150–400 °C. Taking into account that the AC support can lose its weight by reacting with oxygen to emit $CO_2$, the amount of carbon deposition is calculated by the difference in the weight loss between the fresh and the used catalysts in the temperature range of 150–400 °C.[20–22] Based on Fig. 5, the amount of carbon deposition on the used Ru/AC-HNH catalyst is calculated to be 1.9%.

Similarly, the carbon deposition on the other used catalysts was also calculated *via* the corresponding TG and DTG curves (Fig. S1†). As listed in Table 4, for the Ru-based catalysts, the

Table 6 The relative content and binding energy of ruthenium species in the fresh and used catalysts

| | Binding energy (eV), (Area%) | | | |
|---|---|---|---|---|
| Samples | Ru | $RuCl_3$ | $RuO_2$ | $RuO_x$ |
| Fresh Ru/AC | 461.86(14.44) | 463.52(50.52) | 465.04(18.69) | 466.45(16.35) |
| Fresh Ru/AC-$NO_2$ | 461.53(3.95) | 463.22(40.24) | 464.83(31.19) | 466.70(24.62) |
| Fresh Ru/AC-$NH_2$ | 462.10(13.32) | 463.43(47.30) | 465.08(30.37) | 466.66(9.01) |
| Fresh Ru/AC-NHN | 461.67(9.96) | 463.13(35.04) | 464.71(40.22) | 467.03(14.78) |
| Used Ru/AC | 461.31(21.10) | 463.18(46.51) | 464.72(17.44) | 466.59(14.95) |
| Used Ru/AC-$NO_2$ | 461.45(31.88) | 463.14(33.66) | 464.48(28.50) | 466.16(5.96) |
| Used Ru/AC-$NH_2$ | 462.85(24.70) | 463.78(40.38) | 465.15(24.09) | 466.88(10.83) |
| Used Ru/AC-NHN | 462.15(17.69) | 463.30(33.27) | 464.65(35.03) | 466.12(14.01) |

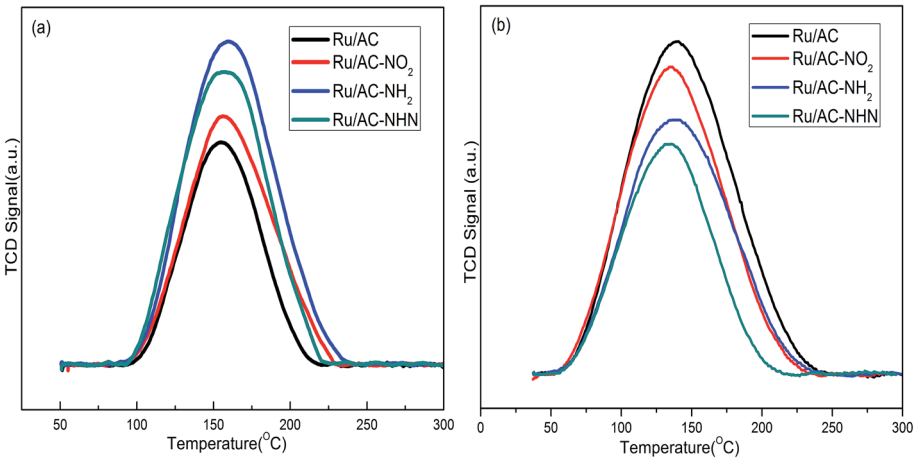


Fig. 7 TPD evolution profiles of the Ru-based catalysts for the desorption of (a) HCl- and (b) $C_2H_3Cl$-.

amount of carbon deposition increases in the order: Ru/AC-NHN (1.9%) < Ru/AC-$NH_2$ (3.2%) < Ru/AC-$NO_2$ (6.8%) < Ru/AC (13.2%). This clearly indicates that the AC support modified by nitrogen functional groups can greatly prevent the coking deposition of the Ru catalyst.

Fig. 6 displays the TPR profiles of the supports and Ru-based catalysts. The broad peak in the range of 500–700 °C for all the samples is attributed to the reduction of oxygenated groups in the carbon support. For the AC-$NO_2$ support, a weak reduction peak appeared in the temperature range of 350–480 °C, which corresponds to the characteristic reduction band of –$NO_2$. However, no obvious peaks appeared in the same temperature range for the other modified carriers. Obviously, there are some $H_2$ consumption peaks in the temperature range of 100–400 °C for all of the Ru-based catalysts, which are due to the reduction of ruthenium species involving the ruthenium oxides and ruthenium chloride in the catalysts. Specifically, for the Ru/AC catalyst, the peak at 138 °C is attributed to the reduction of $RuCl_3$.[23] The Ru/AC-$NO_2$ catalyst exhibits a shoulder peak at 299 °C and a strong peak at 323 °C attributed to the reduction of $Ru^{n+}$ ($n \geq 4$) species.[24] While for the Ru/AC-$NH_2$ catalyst, there are two peaks at 202 °C and 293 °C, which correspond to the reduction peaks of $RuCl_3$ and $RuO_2$, respectively.[25,26] The catalyst Ru/AC-NHN shows a broad peak corresponding to $RuO_2$ at 291 °C. Through comparing the TCD signals with a standard, the fraction of different Ru species existing in these fresh catalysts can be estimated. Calculated from the peak area of TPR, it is worth mentioning that the relative areas of the $H_2$ consumption peaks reduce in the order: Ru/AC (4.16%) < Ru/AC-$NH_2$ (6.64%) < Ru/AC-NHN (20.60%) < Ru/AC-$NO_2$ (68.60%) (Table 5). This suggests that there may exist an interaction between the active species and the supports to influence the ruthenium species content.

To explore the amount and kind of ruthenium species, the XPS deconvolution of Ru $3p_{3/2}$ (Fig. S2 and S3 in ESI†) was used to distinguish the different species, including their binding energy and relative quantity. For both the fresh and used Ru-based catalysts, the Ru XPS spectra were deconvoluted into four peaks at 461.86 eV, 463.52 eV, 465.04 eV and 466.45 eV, corresponding to the species of metallic Ru, $RuCl_3$, $RuO_2$ and $RuO_x$, respectively.[27–29] Table 6 shows the ruthenium species and their relative amounts in the fresh and used Ru-based catalysts. The fresh Ru/AC catalyst consists of 50.52% $RuCl_3$, 18.69% $RuO_2$, 16.35% $RuO_x$ and 14.44% metallic Ru. For the fresh Ru-based catalysts deposited on activated carbon modified by nitrogen functional groups, the content of $RuO_2$ is clearly higher than that of the fresh Ru/AC. The previous work demonstrated that $RuO_2$ is an important active ingredient in acetylene hydrochlorination. The carbon modified by nitrogen functional groups can influence the performance of the resultant catalysts, due to enhanced π bonding in the framework, and promote their electron donor–acceptor properties. However, the detailed reaction mechanism is yet to be explored in future work.

Fig. 7 shows the HCl- and $C_2H_3Cl$-TPD profiles of the Ru-based catalysts. The desorption area corresponds to the amount of adsorbed species on the catalysts, and the desorption temperature reflects the adsorption strength. As seen in Fig. 7a, the HCl desorption peak areas on the Ru-based catalysts loaded on modified activated carbon are larger than those on Ru/AC, while the corresponding desorption temperatures are slightly higher. Fig. 7b shows the desorption of $C_2H_3Cl$ on the Ru-based catalysts. The peak area on Ru/AC-NHN is the smallest compared with the other catalysts, which is beneficial for the acetylene hydrochlorination reaction. This indicates that the catalysts loaded on the modified activated carbon show enhanced adsorption of hydrogen chloride and waning adsorption of vinyl chloride, which promotes higher catalytic activities for the acetylene hydrochlorination reaction (Fig. 1c).

## 4. Conclusion

Ru-based catalysts with different supports were prepared using the incipient wetness impregnation method. To study the change of the AC modified with nitrogen function groups and the effects on the Ru-based catalysts, the characterization techniques XRD, BET, TEM, FT-IR, TPD, TPR and XPS were

used. XPS analysis reveals that the carbon supports modified by nitrogen functional groups can affect the amount of ruthenium species in the catalysts involved in metallic Ru, $RuCl_3$, $RuO_2$ and $RuO_x$, which results in good catalytic activity. The best catalytic performance is achieved over the catalyst Ru/AC-NHN, which is a promising non-mercuric catalyst for acetylene hydrochlorination. The increase in the catalytic activity indicates that the modification using nitrogen functional groups will be beneficial for acetylene hydrochlorination.

## Acknowledgements

This work is supported by the National Basic Research Program of China (973 Program, 2012CB720302), National Natural Science Funds of China (NSFC, U1403294, 21366027), Young Scientific and Technological Innovation Leader of Bingtuan (2015BC001), and the Foundation of Young Scientist in Shihezi University (No. 2013ZRKXJQ03).

## References

1 G. J. Hutchings, *J. Catal.*, 1985, **96**, 292–295.
2 J. Zhang, W. Sheng, C. Guo and W. Li, *RSC Adv.*, 2013, **3**, 21062–21068.
3 G. Li, W. Li, H. Zhang, Y. Pu, M. Sun and J. Zhang, *RSC Adv.*, 2015, **5**, 9002–9008.
4 Y. Pu, J. Zhang, L. Yu, Y. Jin and W. Li, *Appl. Catal., B*, 2014, **488**, 28–36.
5 J. Zhao, J. Xu, J. Xu, T. Zhang, X. Di, J. Ni and X. Li, *Chem. Eng. J.*, 2015, **262**, 1152–1160.
6 J. Zhao, T. Zhang, X. Di, J. Xu, J. Xu, F. Feng, J. Ni and X. Li, *RSC Adv.*, 2015, **5**, 6925–6931.
7 B. Wang, L. Yu, J. Zhang, Y. Pu, H. Zhang and W. Li, *RSC Adv.*, 2014, **4**, 15877–15885.
8 Z. Hasan, M. Tong, B. K. Jung, I. Ahmed, C. Zhong and S. H. Jhung, *J. Phys. Chem. C*, 2014, **118**, 21049–21056.
9 H. Cao, L. Xing, G. Wu, Y. Xie, S. Shi, Y. Zhang, D. Minakatad and J. C. Crittenden, *Appl. Catal., B*, 2014, **146**, 169–176.
10 B. Nkosi, M. D. Adams, N. J. Coville, G. J. Hutchings, M. D. Adams, J. Friedl and F. E. Wagner, *J. Catal.*, 1991, **128**, 366–377.
11 E. Bekyarova, M. E. Itkis, P. Ramesh, C. Berger, M. Sprinkle, W. A. de Heer and R. C. Haddon, *J. Am. Chem. Soc.*, 2009, **131**, 1336–1337.
12 V. Jaiboon, B. Yoosuk and P. Prasassarakich, *Fuel Process. Technol.*, 2014, **128**, 276–282.
13 T. Noguchi, *BBA*, 2014, **1847**, 35–45.
14 M. Yang, T. Yang and M. Wong, *Thin Solid Films*, 2004, **1**, 469–470.
15 C. Moreno-Castilla, M. A. Ferro-Garcia, J. P. Joly, I. Bautista-Toledo, F. Carrasco-Marin and J. Rivera-Utrilla, *Langmuir*, 1995, **11**, 4386–4392.
16 I. Bautista-Toledo, J. Rivera-Utrilla, M. A. Ferro-Garcia and C. Moreno-Castilla, *Carbon*, 1994, **32**, 93–100.
17 H. Qian, F. Han, B. Zhang, Y. Guo, J. Yue and B. Peng, *Carbon*, 2004, **42**, 761–766.
18 P. Gao, A. Wang, X. Wang and T. Zhang, *Catal. Lett.*, 2008, **125**, 289–295.
19 Y. Li, G. Lan, G. Feng, W. Jiang, W. Han, H. Tang and H. Liu, *ChemCatChem*, 2014, **6**, 572–579.
20 S. Wang, B. Shen and Q. Song, *Catal. Lett.*, 2009, **134**, 102–109.
21 L. Wang, F. Wang and J. Wang, *Catal. Commun.*, 2015, **65**, 41–45.
22 H. Zhang, B. Dai, X. Wang, W. Li, Y. Han, J. Gu and J. Zhang, *Green Chem.*, 2013, **15**, 829–836.
23 V. Mazzieri, F. Coloma-Pascual, A. Arcoya, P. C. L'Argentière and N. S. Fígoli, *Appl. Surf. Sci.*, 2003, **210**, 222–230.
24 F. Li, J. Chen, Q. Zhang and Y. Wang, *Green Chem.*, 2008, **10**, 553.
25 S. Guo, X. Pan, H. Gao, Z. Yang, J. Zhao and X. Bao, *Chem.–Eur. J.*, 2010, **16**, 5379–5384.
26 P. G. J. Koopman, A. P. G. Kieboom and H. van Bekkum, *J. Catal.*, 1981, **69**, 172–179.
27 J. L. Gómez de la Fuente, M. V. Martínez-Huerta, S. Rojas, P. Hernández-Fernández, P. Terreros, J. L. G. Fierro and M. A. Peña, *Appl. Catal., B*, 2009, **88**, 505–514.
28 S. Sharma, Z. Hu, P. Zhang, E. W. McFarland and H. Metiu, *J. Catal.*, 2011, **278**, 297–309.
29 J.-H. Ma, Y.-Y. Feng, J. Yu, D. Zhao, A.-J. Wang and B.-Q. Xu, *J. Catal.*, 2010, **275**, 34–44.

 